

DOI: 10.1002/ange.200503102

## Label-Free Biosensing with Hydrogel Microlenses\*\*

Jongseong Kim, Neetu Singh, and L. Andrew Lyon\*

Bioresponsive soft materials, which undergo structural and/or morphological changes in response to a biological stimulus, have been investigated for numerous applications in drug-delivery, tissue-regeneration, bioassay/biosensor, and biomimetic systems.<sup>[1–11]</sup> Simple stimuli-sensitive hydrogels are of interest in a number of fields as they allow the use of external stimuli such as temperature, pH, and photon flux to induce physicochemical changes in the material.<sup>[12–21]</sup> More complex hydrogels that are bioresponsive have been engineered by varying the polymer composition, polymeric structure, and the display of specific functional groups.<sup>[1,2,5,7–9,22,23]</sup> While these materials have been successfully employed for various biological applications such as controlled drug-delivery systems and in tissue engineering,<sup>[1–4]</sup> they are still of enormous interest for developing more sophisticated materials that display more complex responsivities. One potential application of such bioresponsive hydrogels is in biosensing, in which a physicochemical change of a hydrogel is monitored and related to a protein, oligonucleotide, or ligand-binding event.<sup>[5,6,11]</sup>

Our group recently developed hydrogel microlenses in which specific protein-binding events<sup>[11]</sup> were monitored as changes in the focal length of the microlens by brightfield optical microscopy. We observed that the focal length of the microlens could be tuned by multivalent protein binding, where the protein–ligand association formed a cross-linker in the hydrogel network. Herein, we take advantage of that fundamental observation by coupling an antigen/antibody pair directly to the microlens, thereby providing a reversibly switchable cross-link on the microlens. This forms the basis of a new biosensing construct that is reversible and simultaneously acts as the biosensor scaffolding/immobilization architecture, transducer, and amplifier, while providing broad tunability of the concentration of the analyte to which the microlens is sensitive. Furthermore, this construct is exceedingly resistant to false signals due to nonspecific

binding, as the microlens bioresponsivity is dependent on the reversible displacement of protein-to-ligand interactions.

To achieve these goals, we prepared hydrogel microparticles (>1 micron in diameter) composed of poly(*N*-isopropylacrylamide-co-acrylic acid) (pNIPAm-co-AAc) through aqueous free-radical precipitation polymerization. We previously demonstrated that similar particles can be used to create self-assembled arrays of hydrogel microlenses on solid supports.<sup>[11,20,24,25]</sup> To render the microlenses reactive to antibodies, a portion of the AAc groups were used to couple an antigen (biotin, as H<sub>2</sub>N-biotin) and aminobenzophenone (ABP) using EDC and DCC, respectively.<sup>[26]</sup> Functionalization with ABP allows for photochemical tethering of anti-biotin after it is associated to the microlens through native antibody–antigen association. The biotin/ABP-functionalized microlenses were then coulombically assembled onto a 3-aminopropyltrimethoxysilane (APTMS)-functionalized glass substrate to form supported microlenses. Bioresponsive microlenses were then prepared by exposure to a buffered solution of polyclonal anti-biotin, which binds to the microlenses through antibody–antigen interactions. Photochemical ligation of the surface-tethered ABP to the antigen-bound antibody was accomplished by using UV irradiation. Thus, the surface of the microlens is decorated with multiple antibody–antigen-based cross-links, which can then be disrupted by the introduction of free antigen to the surrounding medium. As the antibody is covalently tethered to the surface of the microlens, washing with antigen-free media results in reassembly of the tethered antibody/antigen pairs, thereby providing for a reversible biosensing microlens. This approach is outlined in Scheme 1.

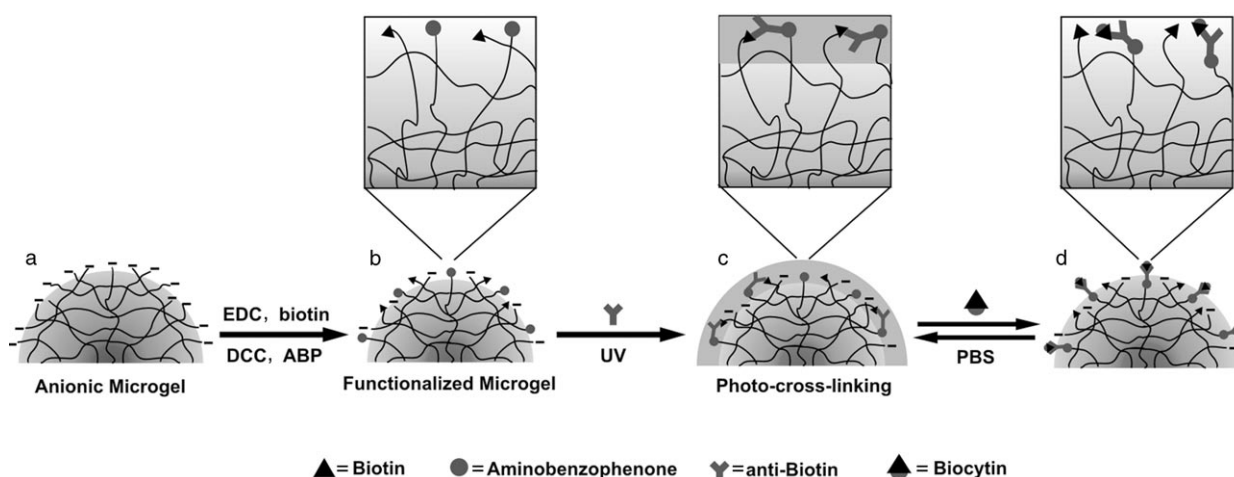
The behavior of the microlenses following incubation with different concentrations of polyclonal anti-biotin is shown in Figure 1a,b. Under these conditions, microlenses not only showed a dependence on the concentration of antibody in the differential interference contrast (DIC) images, with the formation of a dark circle at the particle periphery, but also showed changes in the image projection through the microlenses. The details of image projection through microlenses by optical microscopy have been described previously (see Supporting Information also for a schematic of the microscope setup).<sup>[11,20,24,25]</sup> Above a critical concentration of the antibody the lens is in the “on” configuration, while below that concentration the lens is “off”. These optical effects are a result of the change in the local refractive index (*n*) of the hydrogel microlenses caused by the formation of biotin–anti-biotin cross-links at the surface of the microlens. The critical concentration of anti-biotin represents the point at which the number of cross-linking points is sufficient to cause the microgel periphery to deswell. Below that concentration, the elastic restoring force of the network exceeds the free energy change associated with multivalent antibody binding. In this fashion, the intrinsic binding affinity of the antibody/antigen pair is modulated by the negative entropy associated with gel restriction.

To illustrate the effect of deswelling of the surface of the microlens on the overall optical properties, a series of 2D optical ray-tracing simulations (Raytrace v.2.18) were performed in a medium with *n* = 1.33 (refractive index of water).

[\*] J. Kim, N. Singh, Prof. L. A. Lyon  
School of Chemistry and Biochemistry  
Petit Institute for Bioengineering and Bioscience  
Georgia Institute of Technology  
Atlanta, GA 30332-0400 (USA)  
Fax: (+1) 404-894-7452  
E-mail: lyon@chemistry.gatech.edu

[\*\*] L.A.L. acknowledges support from a Sloan Fellowship and a Camille Dreyfus Teacher–Scholar Award.

Supporting information for this article is available on the WWW under <http://www.angewandte.org> or from the author.



**Scheme 1.** General strategy for label-free biosensing using bioresponsive hydrogel microlenses: a) pNIPAm-co-AAc hydrogel microparticles are assembled as microlenses on a glass substrate; b) conjugation of biotin and ABP to the microlenses; c) assembly of antibodies followed by photochemical ligation; d) reversible displacement of the antibody–antigen cross-link with antigen. EDC = 1-ethyl-3-(3-dimethylaminopropyl)carbodiimide; DCC = dicyclohexyl carbodiimide; PBS = phosphate-buffered saline.

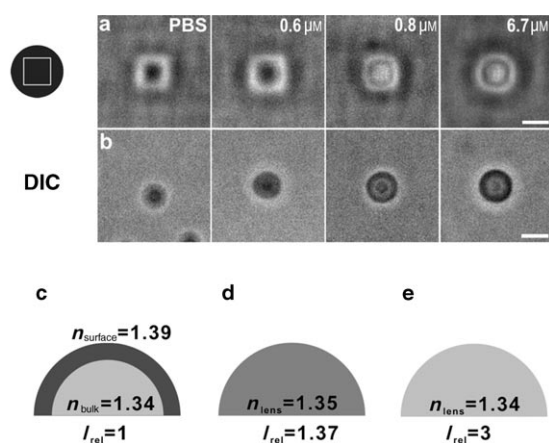


**Figure 1.** Influence of the concentration of polyclonal anti-biotin on lensing and the optical model of the lens structure. a) Projection of a square pattern (shown on left) through a biotin/APB-modified hydrogel microlens upon UV irradiation during incubation with anti-biotin at the concentrations indicated. b) DIC microscopy images taken under the same conditions as in (a). Scale bars: 2  $\mu\text{m}$ . c–e) Results of ray-tracing simulations of the relative focusing powers of the microlens: c) a meniscus + plano-convex compound lens arising from the formation of antibody–antigen cross-links at the microgel periphery; d) a simple plano-convex lens arising from uniform distribution of the two refractive indices in (c); e) a uniform plano-convex lens in the absence of antibody–antigen cross-links. The relevant refractive indices ( $n$ ) and the relative focal lengths ( $l_{\text{rel}}$ ) are indicated. Note that the refractive index of the medium is considered to be  $n = 1.33$ .

In the “on” state of the lens (Figure 1c), the microlens is modeled as a “meniscus + plano-convex” compound lens with a slightly higher refractive index at the periphery ( $n_{\text{surface}} = 1.39$  vs  $n_{\text{bulk}} = 1.34$ ) as a result of a surface-localized binding of biotin to anti-biotin. The simulations show that the compound lens structure produces a significantly shorter relative focal length ( $l_{\text{rel}} = 1.00$ ) as compared to the unmodified hydrogel microlens, which is modeled as a “uniform plano-convex” lens ( $n = 1.34$ ;  $l_{\text{rel}} = 3.00$ ; Figure 1e). In the

compound lens, we have somewhat arbitrarily assumed that antibody–antigen binding, and hence the increase in refractive index, is limited to the outer 25 % of the lens volume ( $\approx 170$  nm deep into the particle). It is clear that the dimensions of the dark circle at the particle periphery are at or below the diffraction limit for visible-light imaging ( $\approx 250$  nm), so this is a reasonable initial estimate. We have also illustrated previously that avidin can diffuse fairly deep into microgels with a similar cross-linking density.<sup>[27]</sup> In Figure 1d, we also compare the surface-localized binding case to a plano-convex lens in which the increase in the refractive index due to antibody–antigen binding is uniformly distributed over the entire optic ( $n = 1.35$ ;  $l_{\text{rel}} = 1.37$ ). In light of the results from the simulation, it is clear that by limiting the hydrogel responsivity to the particle periphery a higher sensitivity to binding events can potentially be obtained as a result of a concomitant localization of the changes in the refractive index. Furthermore, we expect that these structures should display fast response times owing to the short mass-transport distance required to elicit an optical response.

The bioresponsivity of the lens is highly reversible as shown in Figure 2. In this example, the biotin/APB-functionalized hydrogel microlenses were incubated with a solution of polyclonal anti-biotin ( $6.7 \mu\text{M}$ ; equivalent to 670 pmol) and then irradiated with UV light to covalently tether the antigen-associated antibodies to the microlens. The changes in the microlens-projected image were then monitored during exposure to 10 mM PBS (panels a, c, and e) and 1 mM solution of biocytin (panels b, d, and f), which is a water-soluble analogue of biotin. The microlens was initially observed to be in the “on” state in PBS solution which we characterize as the formation of a double-square image in image-projection mode and the dark circle at the particle periphery in the DIC image. Then, when the microlenses were exposed to a solution of free biocytin, they were observed to switch to the “off” state, as characterized by a single square image (projection mode) and the disappearance of the black circle (DIC mode). This change in focal length of the microlens arises from the

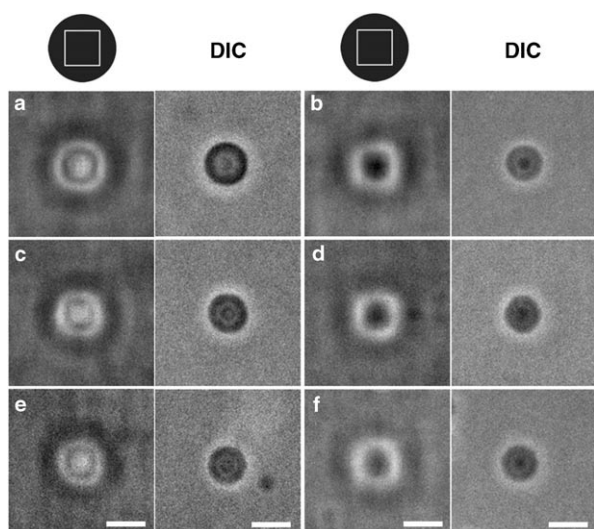


**Figure 2.** Reversibility of the bioresponsive microlenses. In each panel, the left image is the projection of the square pattern and the right image is the DIC image of the microlens. a) Initial “on” state; b) the lens turned “off” with 1 mM biocytin; c, e) the lens reverts to the “on” state upon washing with PBS; d, f) the same conditions as (b), which turns the lens “off”. Scale bars: 2  $\mu\text{m}$ .

disruption of the bound antibody–antigen pairs by competitive displacement with free antigens from solution. When the microlens is returned to an antigen-free buffer, the tethered antibody–antigen pairs reassemble as the free antigens dissociate from the microlens. This response can then be cycled by repeated exposures to either antigen-containing or antigen-free buffer. These results indicate that 1) the microlens response is thermodynamically reversible, that is, the initially photochemically coupled state is a relatively low-energy state, and 2) the antibodies are indeed coupled to the microlens, as reversibility would not be expected if the first displacement interaction led to dissolution of the antibody from the surface of the microlens. Note that this displacement-based mode of action yields microlenses that are insensitive to nonspecific binding as well as specific binding

to non-paratope regions of the tethered antibody (see Supporting Information).

In designing any sensor system, selectivity, sensitivity, and dynamic range are key factors to consider. In light of the results discussed above, we have shown that we can prepare bioresponsive hydrogel microlenses that display high specificity in a label-free format as a result of the use of a displacement/competitive binding scheme. However, the response is essentially a binary (on/off) one that does not allow for quantitative analysis over a wide range of analyte concentrations. Therefore, it should be possible to tune the sensitivity of the microlenses by changing the number of antibody–antigen cross-links present on the microlens, and hence the number that must be displaced to induce a response. This can be trivially accomplished by changing the concentration of polyclonal anti-biotin used in the photochemical cross-linking step to set an initial “on” state of the lens (see Figure 3). As expected, the minimum concentration of biocytin required to switch the microlens state is dependent on the concentration of antibody used in the photochemical cross-linking step. This behavior can be understood by considering the thermodynamics of the system. In the tethered antibody–antigen system, the thermodynamics of hydrogel swelling are intimately coupled with those of the biological affinity pair. That is, the effective affinity of an individual binding pair must be reduced in the case where the gel is deswollen relative to its equilibrium state. Essentially this is a state in which the total free energies of antibody–antigen binding overcome the reduction of network entropy required for deswelling. Thus, there should be a critical number of cross-linking points that result in observable hydrogel deswelling. If the hydrogel microlenses are prepared with excess binding pairs above that critical point, then the individual hydrogel microlenses will reswell only after a suitably large number of displacement events have occurred. However, if the number of cross-linking points is just slightly above this critical point, only a few displacement events will result in gel swelling. Also, note that row (d) shows a lens incubated with 0.6  $\mu\text{M}$  anti-biotin, which is insufficient to turn the lens “on”, even in PBS that is lacking added biocytin.

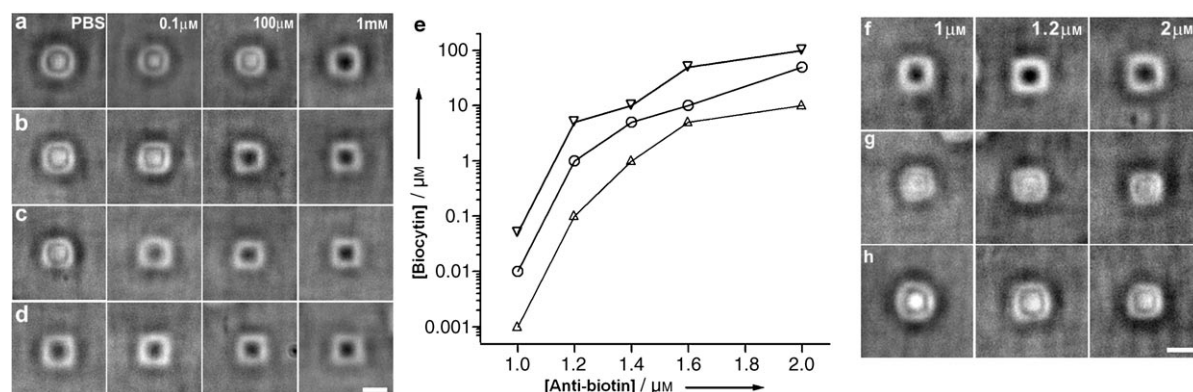


**Figure 3.** Tuning the microlens sensitivity: Row a) projection of the square pattern through a microlens incubated with 6.7  $\mu\text{M}$  anti-biotin before photochemical cross-linking. The biocytin concentrations are indicated at the top of each column. b–d) Incubation with 2  $\mu\text{M}$  anti-biotin (row b), 1  $\mu\text{M}$  anti-biotin (row c), and 0.6  $\mu\text{M}$  anti-biotin (row d). e) Graph of the microlens focusing “state” as a function of the concentration of the solution of biocytin and the initial concentration of anti-biotin.  $\Delta$ : fully “on” state (as shown in row f),  $\circ$ : transition point (row g),  $\nabla$ : fully “off” state (row h). Note that 150  $\mu\text{L}$  of each biocytin solution was used for this experiment (10 nM is equivalent to 1.5 pmol). Scale bars: 2  $\mu\text{m}$ .



These results suggest that the digital nature of an individual microlens response can be overcome by creating microlens arrays in which the individual array elements exhibit differing analyte sensitivities.

To observe microlens switching in more detail, we exposed the hydrogel microlenses to a narrower range of biocytin concentrations (Figure 3e and f). These experiments reveal that hydrogel microlenses show at least three distinct image projection modes, which we refer to here as “off”, “intermediate”, and “on”, in response to different concentrations of anti-biotin (Figure 3f–h). Figure 3e shows the occurrence of each state upon changing the biocytin concentration as a function of the initial concentration of anti-biotin. From these data it is clear that the bioresponsive microlenses do display a transition range of finite width and are hence not purely binary response elements, thereby coupling the ultimate sensitivity of the element with our ability to observe subtle changes in microlens focal length. Most importantly, Figure 3e shows a modulation of microlens sensitivity over approximately four orders of magnitude, clearly illustrating the potential for using gel-swelling thermodynamics to modulate the sensitivity of a bioaffinity-based sensor element.

In conclusion, we have demonstrated a new approach to label-free biosensing by combining antibody–antigen cross-linked hydrogel microlenses with a simple brightfield optical microscopy technique. The utility of the construct for the detection of small molecules, its resistance to interferences from nonspecific adsorption, the ability to tune the sensitivity, the requirement of only a small volume of the sample, and the inexpensive, rapid, and simple fabrication method make this a potentially powerful and general biosensing construct. Furthermore, these fundamental advantages make this material attractive for the future development of bioresponsive materials in applications far beyond bioanalysis.

Received: August 31, 2005

Published online: January 27, 2006

**Keywords:** antibodies · antigens · biosensors · gels · polymers

- [1] B. Jeong, Y. H. Bae, D. S. Lee, S. W. Kim, *Nature* **1997**, 388, 860.
- [2] P. F. Kiser, G. Wilson, D. Needham, *Nature* **1998**, 394, 459.
- [3] R. Langer, *Nature* **1998**, 392, 5.
- [4] M. P. Lutolf, J. L. Lauer-Fields, H. G. Schmoekel, A. T. Metters, F. E. Weber, G. B. Fields, J. A. Hubbell, *Proc. Natl. Acad. Sci. USA* **2003**, 100, 5413.
- [5] T. Miyata, N. Asami, T. Urugami, *Nature* **1999**, 399, 766.
- [6] J. H. Holtz, S. A. Asher, *Nature* **1997**, 389, 829.
- [7] C. Wang, R. J. Stewart, J. Kopecek, *Nature* **1999**, 397, 417.
- [8] A. Aggeli, M. Bell, N. Boden, J. N. Keen, P. F. Knowles, T. C. McLeish, M. Pitkeathly, S. E. Radford, *Nature* **1997**, 386, 259.
- [9] K. N. Plunkett, K. L. Berkowski, J. S. Moore, *Biomacromolecules* **2005**, 6, 632.
- [10] D. G. Anderson, J. A. Nurdick, R. Langer, *Science* **2004**, 305, 1923.
- [11] J. Kim, S. Nayak, L. A. Lyon, *J. Am. Chem. Soc.* **2005**, 127, 9588.
- [12] K. Dusek, K. Patterson, *J. Polym. Sci. Polym. Phys. Ed.* **1968**, 6, 1209.
- [13] T. Tanaka, D. J. Fillmore, *J. Chem. Phys.* **1979**, 70, 1214.
- [14] B. R. Saunders, B. Vincent, *Adv. Colloid Interface Sci.* **1999**, 80, 1.
- [15] R. Pelton, *Adv. Colloid Interface Sci.* **2000**, 85, 1.
- [16] M. Arotcarena, B. Heise, S. Ishaya, A. Laschewsky, *J. Am. Chem. Soc.* **2002**, 124, 3787.
- [17] V. T. Pinkrah, A. E. Beezer, B. Z. Chowdhry, L. H. Gracia, J. C. Mitchell, M. J. Snowden, *Langmuir* **2004**, 20, 8531.
- [18] M. Bradley, B. Vincent, *Langmuir* **2005**, 21, 8630.
- [19] Y. Luo, M. S. Shoichet, *Nat. Mater.* **2004**, 3, 249.
- [20] J. Kim, M. J. Serpe, L. A. Lyon, *J. Am. Chem. Soc.* **2004**, 126, 9512.
- [21] I. Berndt, J. S. Pedersen, W. Richtering, *J. Am. Chem. Soc.* **2005**, 127, 9372.
- [22] K. Dusek, M. Duskova-Smrckova, M. Ilavsky, R. Stewart, J. Kopecek, *Biomacromolecules* **2003**, 4, 1818.
- [23] S. Nayak, H. Lee, J. Chmielewski, L. A. Lyon, *J. Am. Chem. Soc.* **2004**, 126, 10258.
- [24] M. J. Serpe, J. Kim, L. A. Lyon, *Adv. Mater.* **2004**, 16, 184.
- [25] J. Kim, M. J. Serpe, L. A. Lyon, *Angew. Chem. Int. Ed.* **2005**, 44, 1333; *Angew. Chem.* **2005**, 117, 1357.
- [26] G. T. Hermanson, *Bioconjugate Techniques*, Academic Press, San Diego, **1996**.
- [27] S. Nayak, L. A. Lyon, *Angew. Chem. Int. Ed.* **2004**, 43, 6706; *Angew. Chem.* **2004**, 116, 6874.